Supplementary information

Two-Dimensional Carbon Networks with a Negative Poisson's Ratio

Hao Yuan[1,2], Guan Huang [1,2], Guangzhao Qin[3], Li-Chuan Zhang[1,2,*], Yuee Xie[1,2,*] and YuanPing Chen [1,2,*]

1 School of Physics and Electronic Engineering, Jiangsu University, Zhenjiang 212013, China
2 Jiangsu Engineering Research Center on Quantum Perception and Intelligent Detection of Agricultural Information, Zhenjiang 212013, China
3 State Key Laboratory of Advanced Design and Manufacturing for Vehicle Body, College of Mechanical and Vehicle Engineering, Hunan University, Changsha 410082, China
* Correspondence: lichuan.zhang@ujs.edu.cn (L.Z.); yueex@ujs.edu.cn (Y.X.); chenyp@ujs.edu.cn (Y.C.)

1. The negative Poisson's ratio (NPR) in graphene

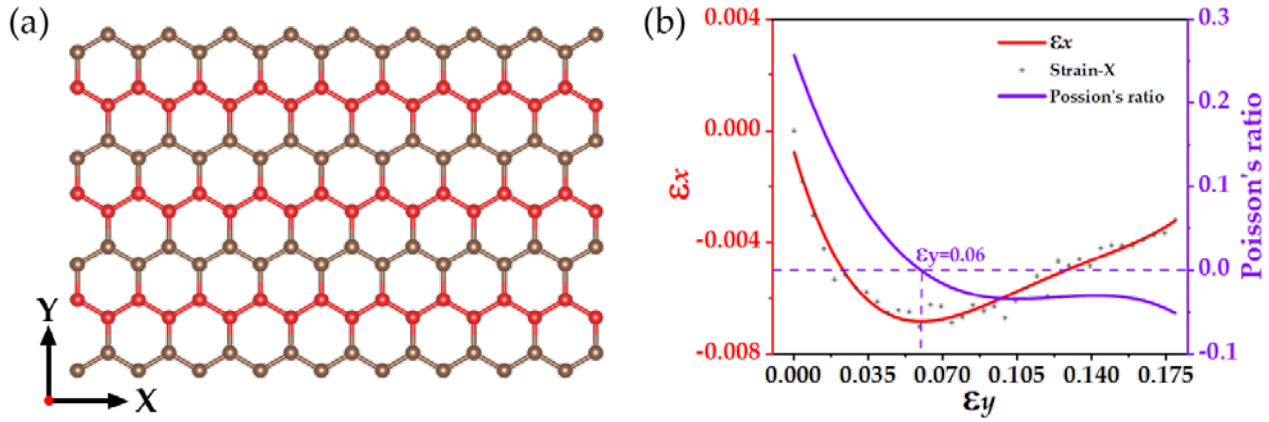

Figure S1. (a) The schematic structure of graphene. Here, the zigzag chain is marked with two different colors. (b)The mechanical response of graphene. the red line indicates the ε_x-ε_y curve under the uniaxial strain along the *y*-direction, and the purple line represents Poisson's ratio under the uniaxial strain along the *y* direction. The purple dotted line represents the zero Poisson's ratio.

The NPR is observed when $\varepsilon_y > 0.06$, which is consistent with the findings of other researchers [46], demonstrating the reliability of the Airebo potential function.

2. The video for stretch of zigzag carbon chains

We used the Airebo potential function together with Lammps package to simulate the mechanical response of the carbon chain when the vertical stretch is applied. The video of the stretching process is available in the zip file, named Zigzag-Chain.mp4.

3. The phonon dispersions of eight 2D carbon structures C12, C10, C16 , C32, C20, C14, C24, C36

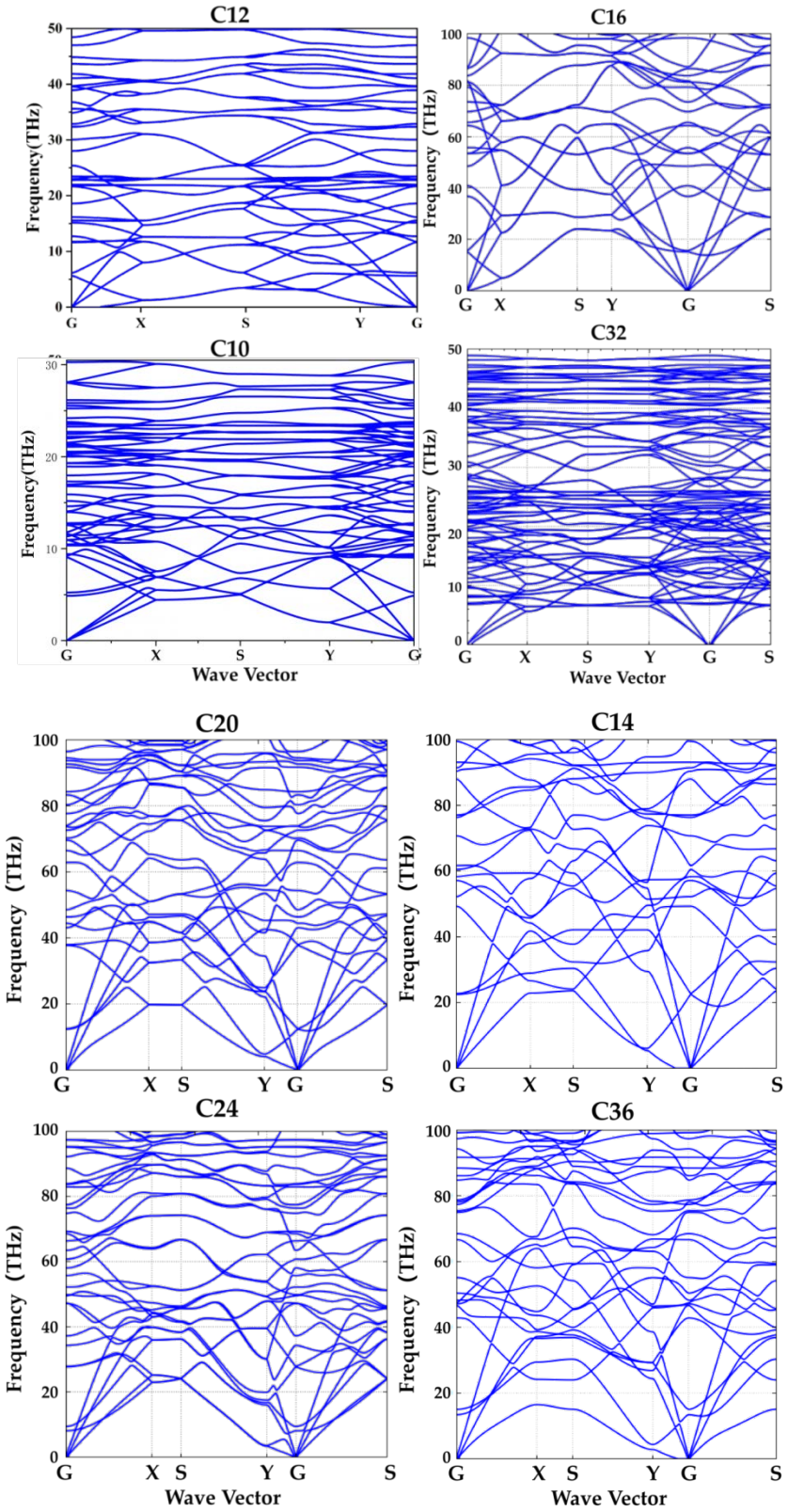

Figure S2. The phonon dispersion of four structures C12, C16, C10, and C32. The Brillouin zone of these four structures is rectangular, and the phonon dispersion profile show positive values along G-X-S-Y-G. The phonon dispersion of four structures C20, C14, C24, and C36. The Brillouin zone of these four structures is rectangular, and the phonon dispersion profile show positive values along G-X-S-Y-G-S.

4. Structure parameters of C12, C10, and C14

Table S1. Structure parameters of C12, C10, and C14 with the initial case; the case for the appearance of NPR, and the case when 11% stretch is applied. Bond angles and bond lengths of these structures are marked with α, β, γ and l, m, n, j in Figure 3 of the manuscript.

Status	*Initial state*			*NPR appears*			*NPR state (11%)*		
No	**C12**	**C10**	**C14**	**C12**	**C10**	**C14**	**C12**	**C10**	**C14**
α	α_1=112.42°	α_2=118.23°	α_3=115.78°	α_4=108.64°	α_5=114.57°	α_6=112.90°	α_4=107.26°	α_5=112.38°	α_6=110.95°
β	β_1=112.42°	β_2=121.76°	β_3=112.16°	β_4=108.64°	β_5=117.32°	β_6=110.48°	β_4=107.26°	β_5=115.86°	β_6=108.63°
γ	γ_1=121.85°	γ_2=118.23°	γ_3=115.78°	γ_4=116.85°	γ_5=114.57°	γ_6=112.90°	γ_4=115.35°	γ_5=112.38°	γ_6=110.95°
l	l_1=1.435Å	l_2=1.421Å	l_3=1.396Å	l_4=1.432Å	l_5=1.421Å	l_6=1.382Å	l_4=1.448Å	l_5=1.455Å	l_6=1.400Å
m	m_1= 1.421Å	m_2=1.426Å	m_3=1.381Å	m_4=1.458Å	m_5=1.412Å	m_6=1.396Å	m_4=1.474Å	m_5=1.427Å	m_6=1.419Å
n	n_1=1.435Å	n_2=1.426Å	n_3=1.381Å	n_4=1.432Å	n_5=1.412Å	n_6=1.396Å	n_4=1.448Å	n_5=1.427Å	n_6=1.419Å
j	j_1=1.426Å	j_2=1.421Å	j_3=1.396Å	j_4=1.395Å	j_5=1.421Å	j_6=1.382Å	j_4=1.413Å	j_5=1.455Å	j_6=1.396Å

In Table S1, the changes of the three two-dimensional carbon structures C12, C10 and C14 under mechanical response are sorted out, which are respectively the initial state, the state of NPR appears and the state of NPR state (11%). As can be seen from the table, the length of the bond decreases first and then increases as the response changes. And the bond Angle is decreasing all the time.

Table S2. The average bond lengths and bond angles for structures C12, C10, C14, C36, C20, and C24, and no external strain is applied.

Label	*Average θ(°)*	*Average d(Å)*	*Label*	*Average θ(°)*	*Average d(Å)*
C12	115.565°	1.42993Å	C36	115.38°	1.3775Å
C10	118.182°	1.42202Å	C20	113.79°	1.3733Å
C14	115.777°	1.38853Å	C24	113.04°	1.3660Å

As can be seen from Table S2, when NPR occurs in these structures, C12, C10 and C14, their bond angles are basically within the range of bond angles mentioned in the model in Figure 2, which is one of the reasons why C36, C20 and C24 appear NPR later than the above three structures. It can also be found from the bond length of the six structures that C36, C20 and C24 are smaller than the bond length (1.42 Å) when the serrated carbon chain generates NPR, so it appears later on NPR.

5. The mechanical response of C12, C10, C14, C36, C20, C24 under the uniaxial stretch along *x* direction.

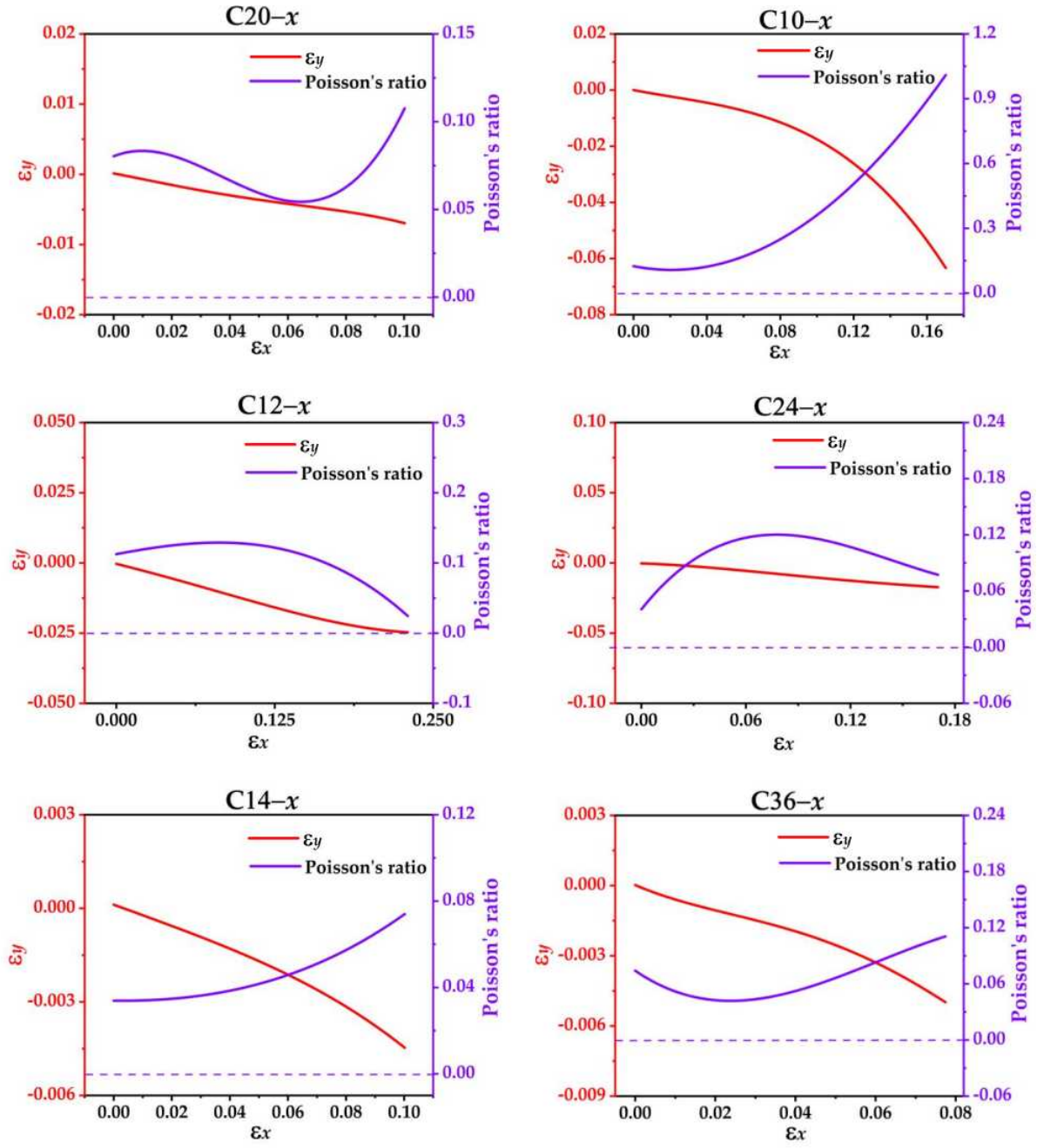

Figure S3. The mechanical response of C12, C10, C14, C36, C20, C24 under the uniaxial strain along the x-axis. The red line indicates the response of the driven strain under the uniaxial strain along the x-axis, and the purple line represents the Poisson's ratio under the uniaxial strain along the y direction. The purple dashed line indicating the zero Poisson's ratio state.

6. Poisson's ratio curve and strain curve of C10 at 300K and 10K temperature

To explore the influence of temperature, we performed molecular dynamics simulations at 300 K for the structure C10 (one structure in Figure 3). As shown in supplementary S6, we find that the temperature does influence the occurrence of negative Poisson's ratio and the value of Poisson's ratio. Besides, compared to the case of T=10K, the absolute value of Poisson's ratio decreases with the increase of temperate. this phenomenon is consistent with the case of graphene [50], which may be aroused by the weaker quantum effect at high temperature.

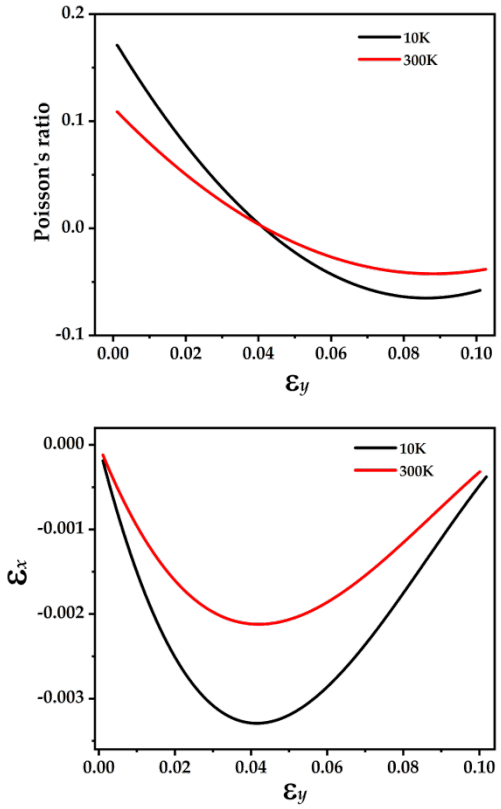

Figure S4. Poisson's ratio curves and strain curves of C10, at the temperature of 300K and 10K.

7. The comparison of effective elastic constants calculated by DFT and MD methods.

In two-dimensional systems, the calculated elastic constants should be rescaled by multiplying a coefficient z/t to obtain the real results, which can be defined as effective elastic constants [61], where z is the vacuum layer of the system (20 Å) and t is the effective thickness of systems (3.5 Å). The effective elastic constants calculated by MD with Airebo function and DFT methods for C10, C12, C14, and graphene are shown in Table S3. From Table S3, we can find that the main difference between the DFT and MD results is the elastic constant C_{12}.

Table S3. The effective elastic constants of C10, C12, C14, and graphene according to the MD with Airebo function and DFT calculations.

No	Airebo				DFT			
	C12	C10	C14	graphene	C12	C10	C14	graphene
C_{11} (GPa)	828.060	908.02	986.99	913.214	764.060	850.8	898.17	1011.37
C_{12} (GPa)	63.110	46.78	20.19	335.130	184.220	189.43	167.66	177.98
C_{22} (GPa)	961.580	1013.2	1013.829	913.214	958.350	916.9	953.26	1011.37
C_{66} (GPa)	315.430	480.46	492.70	289.040	279.810	315.6	322.97	416.69

8. Poisson's ratio of graphene, C10, and C16 calculated by DFT method.

As shown in Figure S5, under the tensile strain along the *y*-axis, NPR occurs first in the C10 system rather than graphene, and the C16 system doesn't have NPR until the structure is broken, which is consistent with the results of MD.

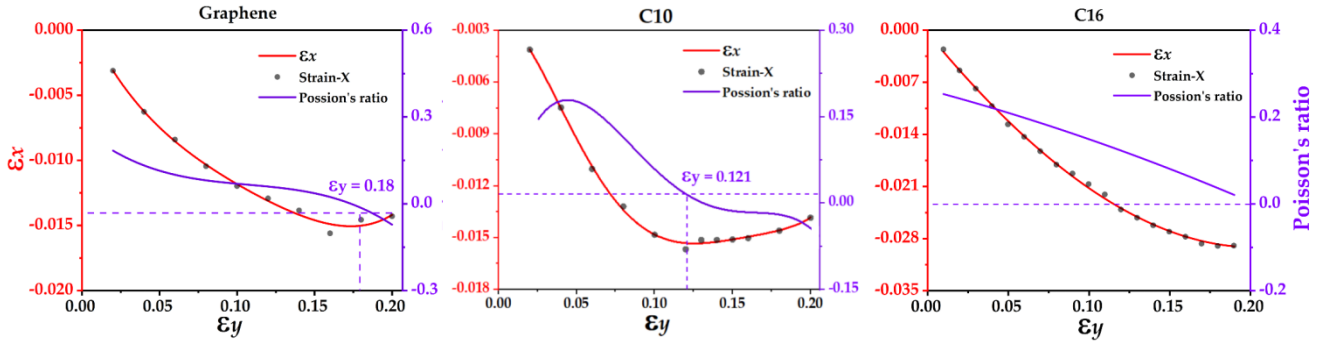

Figure S5. The result of mechanical responses of structures graphene, C10, and C16 according to DFT calculations. The red line indicates the response of the driven strain under the uniaxial strain along the *y*-axis, and the purple line represents Poisson's ratio under the uniaxial strain along the *y*-axis.